Polímeros
ISSN 1678-5169 (Online)

https://doi.org/10.1590/0104-1428.202400636

ORIGINAL ARTICLES

Rheo-optical characterization of polymer chain uncoil and disentanglement in shear flow

Murilo Tambolim[1] and Sebastião Vicente Canevarolo[2]*

[1]Programa de Pós-graduação em Ciência e Engenharia de Materiais – PPGCEM, Universidade Federal de São Carlos - UFSCar, São Carlos, SP, Brasil

[2]Departamento de Engenharia de Materiais – DEMa, Universidade Federal de São Carlos – UFSCar, São Carlos, SP, Brasil

**caneva@ufscar.com.br*

Abstract

Rheo-optical studies allow the monitoring of rheological properties by indirect measurements of optical properties. For pure polymeric fluids, flow birefringence can be used to quantify the molecular orientation level by the application of shear strain rates. In this work, flow birefringence experiments were carried out with a pure polystyrene under different shear rates, shear cycles, and temperature conditions, in a polarized light optical microscope under controlled shear. The level of orientation and its correlation with the dynamics of uncoil/recoil and disentanglement were analyzed. The expected increase in the orientation level as a function of the increase in the shear rate due to the chain uncoiling was confirmed. Following, the chain orientation level reduces over time, associated with chain disentanglement and its subsequent recoiling. Disentanglement behaves irreversibly, while uncoiling and recoiling are reversible processes. A model is proposed to represent these dynamics.

Keywords: *disentanglement, polymer chain orientation, flow birefringence, rheo-optical measurement, polystyrene.*

How to cite: Tambolim, M., & Canevarolo, S. V. (2024). Rheo-optical characterization of polymer chain uncoil and disentanglement in shear flow. *Polímeros: Ciência e Tecnologia*, *34*(4), e20240038. https://doi.org/10.1590/0104-1428.202400636

1. Introduction

Rheo-optics techniques jointly address the rheology of polymers and their optical properties, such as birefringence. Flow birefringence can be used to quantify chain orientation level, due to the anisotropy of polymer chains[1-5]. A relevant concept in polymer rheology is the dynamics of uncoiling/recoiling and disentanglement/reentanglement of chains during their orientation process under melt flow.

The first theories of molecular chain motions were developed by Rouse[6], Bueche[7], Zimm[8] and Peticolas[9] in the 1950s and 1960s, in which polymer chains are considered as a succession of equal submolecules, represented by a sequence of spheres connected by springs. This model is useful for polymer solutions with low concentration. For polymer flow in the melt state, the understanding of the entanglement concept is fundamental. This concept emerged in the 1930s[10] and has been an important topic ever since[11-18]. The de Gennes'[19] chain reptation model is one of the most adopted theories to correlate properties of polymeric fluids in the presence of entanglements. It assumes that the chain motion is restricted by entanglements, as if the chain was inside a tube, and the reptation mechanism allows the molecule to slip inside it.

There are several studies to develop methods to disentangle polymer chains, such as during the polymerization, under polymer solution, etc. Disentangling chains in the molten or softened state was first proposed by Ibar[20,21]. The development of grades with prior disentanglement treatment is interesting to achieve lower viscosities during processing and, thefore, better processability, especially for polymers with high molecular weight. It is known that high levels of disentanglemnt are possible to be obtained when applying shear rates for a long period, just as it is expected that the disentanglement rate decreases over time[20-23]. In 2018, Li and Matsuba[24] proposed that the higher level of entanglement is responsible for preserving molecular orientation in shear flow. Wattanabe et al.[25] and Noirez et al.[26] studies challenged the assumptions that flow shear thinning of entangled polymer chains is due to significant orientation of the segments between the entanglements under shear flow. In their studies, both concluded that the chains remained largely undeformed under steady-state shear flow conditions for which extensive shear thinning was present. These results also represent a challenge for the reptation model. Wang et al.[27] experimentally demonstrated that the chain retraction step of the tube model does not occur, which led to the conclusion that the current understanding of the flow and relaxation of entangled polymers based on the theoretical reptation model is limited.

The reentanglement effect is a much slower process. Roy and Roland[28] studied the process of reentangling polyisobutylene, it was more than an order of magnitude slower than expectations based on the linear relaxation

time of the fully entangled material. Ibar[29] concluded that the recovery time of untangled PMMA treated by the so-called shear strengthening machine was 17 million times greater than its longest relaxation time (5 ms). Fu et al. [30] showed that higher shear rates induce higher levels of disentanglement, resulting in up to 93.7% lower viscosity, greater molar mass between entanglements, and longer reentanglement time.

The objective of this work is, by using flow birefringence optical measurement of a polystyrene (PS) during shearing flow, correlate it with the level of orientation of the chains, and propose a model for the dynamics of uncoiling, disentanglement and recoiling. The experiments are carried out in a shearing parallel plate system (CSS450) with temperature and shear rate control, fitted in a polarized light optical microscope, and a homemade optical detector for quantifying the cross polarized transmitted light intensity through the soften polymer to get the flow birefringence. The measurements were done under different shearing conditions, varing its maximum value, sequence and time of disentanglement shearing treatment, and temperature. With that, a model have been proposed for molecular chain disentanglement and recoiling.

2. Materials and Methods

Pure GPPS N 2560 from Innova was used. It is a pure atactic homopolystyrene with high molar mass ($M_w \cong 260.000$ g/mol, $M_n \cong 140.000$ g/mol). Polystyrene shows negative birefringence, high polarizability and intrinsic birefringence for completely oriented chains of $\Delta n \cong -0.1 = -1,000 \times 10^{-4}$[31].

The rheo-optical characterization of the polymer was carried out using a Leica DMRXP polarized light optical microscope (MOLP), with attachment of an Cambridge Shearing System CSS450 accessory from Linkam Scientific Instruments and an optical detector made of a light dependent resistor LDR, placed in the microscope optical tube, partially covered to reduce the sample measuring area and so unwanted changes in the shear rate. This sensor is set after the analyzer polarization filter. The cross polarized transmitted light intensity signal I, measured by the LDR, is normalized ($0 \le I_N \le 1$) using Equation 1, converted into Optical Path Difference (OPD) using Equation 2, and finally converted into flow birefringence (Δn) using Equation 3, knowing the sample film thickness.

$$I_N = \frac{I - I_C}{I_P - I_C} \tag{1}$$

$$I_N = \frac{1}{2}\left(1 - \frac{\cos\left(2\pi OPD/\lambda\right)}{\cosh(\beta 2\pi OPD/\lambda)}\right) \tag{2}$$

$$\Delta n = \frac{OPD}{t} \tag{3}$$

being I_C the transmitted light intensity with polarizers set crossed (minimum intensity), I_P the transmitted light intensity with polarizers set parallels (maximum intensity), $\lambda = 550$ nm the average wavelength of the white light, β the damping coefficient, and $t = 400$ μm the sample thickness. The data is collected at a frequency of 5 Hz by a software written in LabVIEW 8.6, developed inhouse[32], and edited as needed to better suit these measurements.

The normalized cross polarized transmitted light intensity I_N, measured by the optical detector was calibrated using a Berek compensator B containing a tilting magnesium fluoride MgF_2 plate[33], measurements taken every 0.1º tilting degree, in both directions (named black and red scales), up to 4 light interference orders. The two curves were shifted to minimize the uncertainty of the compensator screw drum at OPD = Zero nm. By tilting the crystal an angle i, a phase difference δ (nm) is introduced in the optical path, following Equation 4[33]:

$$\delta = tn_o\left(\sqrt{1 - \frac{\sin^2 i}{n_e^2}} - \sqrt{1 - \frac{\sin^2 i}{n_o^2}}\right) \tag{4}$$

being, t the crystal thickness ($1.525 \ \ 10^6$ nm), $n_o = 1.37859$ and $n_e = 1.39043$ the ordinary and extraordinary refractive indices of the MgF_2 crystal respectively, given an intrinsic birefringence of $\Delta n = n_e - n_o = 118.4 \times 10^{-4}$, measured by a monochromatic light with $\lambda = 546.1$ nm (e line).

Two different shearing procedures were applied, using 0.27 g of the material in melt state. (1) **Shearing scan**: Shear the sample from $0.01\ s^{-1} \le \dot{\gamma} \le 180\ s^{-1}$ (reaching the maximum shear rate of the equipment for the fixed sample thickness of 400 μm, set by the gap between the quartz plates), in a profile of 20 steps distributed on a log scale values, holding 60 seconds at each one to collect the signal and average it to get I_N. Various isothermal scans in the range of $180℃ \le T \le 230$ ℃ were tested. (2) **Disentanglement shearing treatment**: The sample, starting at rest, is rapidly sheared (time ≤ 1 min) with increasing shear rates up to $\dot{\gamma} = 180\ s^{-1}$ at 180℃. The rise in shear rate is done quickly to minimize the unwanted pre-disentanglement of the chains. Then the sample is kept at a constant $\dot{\gamma} = 180\ s^{-1}$ for a preset shearing time (2, 5 and 60 min, as indicated). The data is collected at 5 Hz and displayed.

2.1 Increase in the molecular chain orientation level during shearing scan

The sample was subjected to the shearing scan profile at 180 °C. This temperature was set under preliminary measurements at which a balance of high flow birefringence values and good melt flow stability is obtained for the PS used. The normalized intensity I_N, optical path difference OPD and flow birefringence Δn as a function of the shear rate $\dot{\gamma}$ were calculated and displayed.

2.2 Reduction in the molecular chain orientation level during disentanglement shearing treatment

The sample at 180 °C is rapidly sheared from rest up to $\dot{\gamma} = 180\,s^{-1}$. The polymer chains are disentangled by keeping the shear rate $\dot{\gamma} = 180\,s^{-}$ constant during 60 min. The curve of I_N as a function of time is obtained to monitor the changes in the level of chain orientation, revealed as flow birefringence.

2.3 Reduction in the molecular chain orientation level during sequential runs of disentanglement shearing treatments

The effect of cumulative chain disentanglement levels in the material was quantified by cycling up to three sequential shearing scans at 180 °C. Each cycle is done by the following steps: 1) fast shear rate increase up to $\dot{\gamma} = 180 s^{-1}$; 2) 60 min disentanglement shearing treatment at constant shear rate of $\dot{\gamma} = 180 s^{-1}$; 3) fast shear rate reduction down to rest; and 4) 1 min rest. After resting, a new cycle is applied. During each complete cycle, I_N, OPD and Δn as a function of $\dot{\gamma}$ were calculated.

2.4 Molecular chain orientation level after sequential disentanglement shearing treatment runs

Four shearing scans followed by disentanglement shearing treatment were applied sequentially at 180 °C. The sequence was performed twice, for 2 and 5 min disentanglement shearing treatment times. Flow birefringence Δn as a function of shear rate $\dot{\gamma}$ was calculated and displayed.

2.5 Molecular chain orientation level as a function of melt shearing temperature

Shear scans were applied for melt temperatures of 180, 190, 200, 210, 220 and 230 °C, either without applying previous disentanglement or after applying 60 min shearing disentanglement treatment, by using different samples. I_N, OPD and Δn as a function of $\dot{\gamma}$ were calculated. By fitting straight lines in the initial portion of the Δn *vs* $\dot{\gamma}$ curves ($1\times10^{-4} < -\Delta n < 4\times10^{-4}$), their extrapolation to $\Delta n = 0$ leads to the polymer average relaxation time λ_r as Equation 5.

$$\lambda_r = 1/\dot{\gamma}_{\Delta n \to 0} \quad (5)$$

3. Results and Discussions

3.1 Optical detector calibration

Figure 1 shows the normalized cross polarized transmitted light intensity I_N experimental points (black and red) measured by inserting the Berek compensator B in the light path and the best fitting theoretical curve (continuous green line), which by applying Equation 2, one gets coefficient $\beta = 0.12$. The experimental data follows closely the expected theoretical curve, confirming the efficiency of the optical arrangement for quantitative measurements.

3.2 Increase in the molecular chain orientation level during shearing scan

Figure 2 shows the curve of normalized cross-polarized transmitted light intensity I_N as a function of shear rate $\dot{\gamma}$ applied to the PS sample at 180 °C. The maximum I_N value (0.95) is obtained at $\dot{\gamma} = 8.8\ s^{-1}$, revealing the half of the first light interference order, i.e. an OPD = 275 nm. The end of the first order occurs approximately at 20 to 30 s^{-1} for a I_N close to 0.30 to 0.40, for an OPD = 550 nm. Half of the second order occurs at approximately 60 to 100 s^{-1} and I_N close to 0.80 to 0.90, for an OPD = 825 nm. At the maximum measurable shear rate delivered by the equipment $\dot{\gamma} = 180 s^{-1}$, the I_N obtained is 0.58, lying between the middle and the end of the second order.

The curve of birefringence Δn as a function of shear rate $\dot{\gamma}$ applied is shown in Figure 3. It establishes a more direct correlation with the orientation level. At shear rates high enough to overcome the effect of molecular chain relaxation, the chains uncoil themselves and orient along the direction of stress, resulting in $-\Delta n > 0$. Increasing further $\dot{\gamma}$ leads to higher $-\Delta n$ values, that is, higher molecular chain orientation levels, as expected. The results are similar to those got by Vasconcelos'[34], which were obtained for the same material and equipment, but at 210 °C.

3.3 Reduction in the molecular chain orientation level during disentanglement shearing treatment

I_N as a function of disentanglement shearing treatment time at $180 s^{-1}$ and 180 °C for up to 60 minutes is presented in Figure 4. In the same figure, there is a miniature representation of Figure 2 at the top right, to support the interpretation. The initial I_N value is 0.64 , given a $\Delta n = -23.3\times10^{-4}$, i.e. ~43 times lower than the intrinsic birefringence of polystyrene ($\Delta n = -1,000\times10^{-4}$) and ~75 times lower than the calcite crystal ($\Delta n = -1,720*10^{-4}$). The value is close to that obtained in Figure 2 at 180 s^{-1}, as expected. During the 60 min treatment, I_N reduces towards values that would be

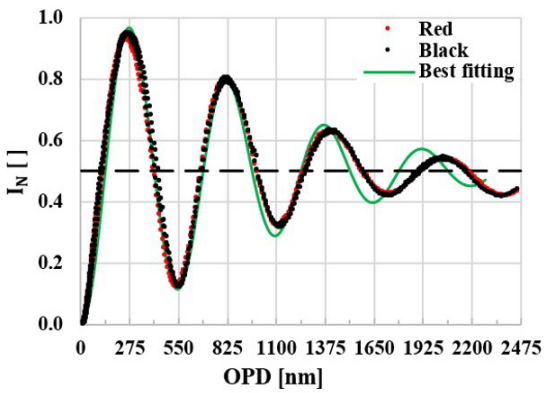

Figure 1. Calibration curve of normalized cross polarized transmitted light intensity I_N as a function of optical path difference OPD, done by using a Berek compensator B.

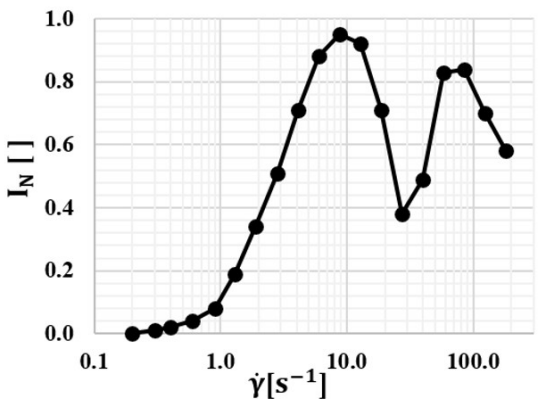

Figure 2. The normalized cross-polarized transmitted light intensity I_N of polystyrene as a function of shear rate $\dot{\gamma}$ at 180 °C.

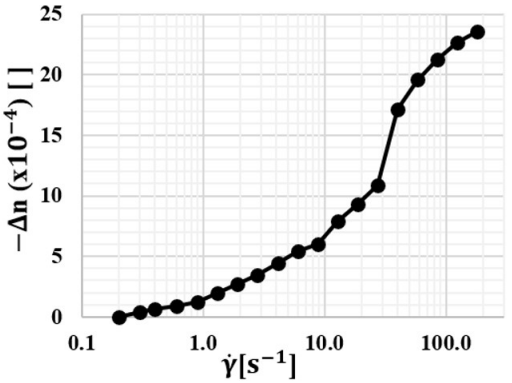

Figure 3. Flow birefringence -Δn of polystyrene as a function of shear rate $\dot{\gamma}$ at 180 °C. Δn reaches -23.3×10^{-4} at $180\,s^{-1}$.

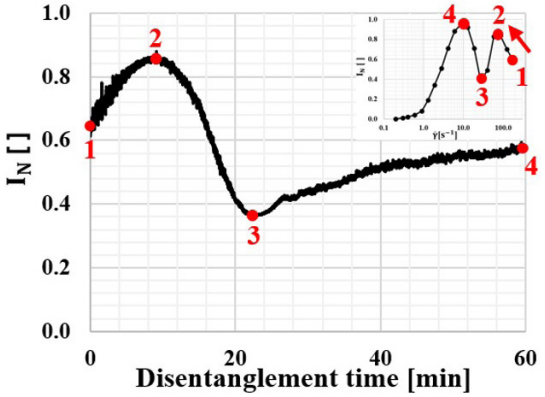

Figure 4. Changes in the normalized cross-polarized transmitted light intensity I_N as a function of time during polystyrene disentanglement shearing treatment at 180 °C and 180 s^{-1}. After 60 min the flow birefringence of polystyrene reduces to $\Delta n = -3.7\times10^{-4}$.

obtained at lower $\dot{\gamma}$ values, which can be easily interpreted by following the curve presented in the miniature insert. Therefore, the molecular chain orientation level reduces over time. At the end of the experiment, $I_N = 0.57$, setting its OPD in between the half and end of the first light interference order and, reaching a $\Delta n = -3.7\times10^{-4}$, ~84% lower than the initial value.

Maintaining a constant shear rate $\dot{\gamma}$, the reptation motion allows entangled chain segments that are closer to their chain ends to disentangle more easily. Gradually lower levels of entanglement are expected, as observed by Buchdahl[13] and Ibar[20,21]. The disentanglement leads to an increase in the conformational freedom of the chain, facilitating its partial recoiling, resulting in a gradual reduction in the orientation level over time. This dependence of the orientation on the entanglement level was also observed by Li and Matsuba[24]. The lower orientation level of the chain segments reduces the ability of the chains to disentangle, as they are in a more relaxed state. Therefore, the molecular chain disentanglement rate decreases over time, leading eventually to its stabilization.

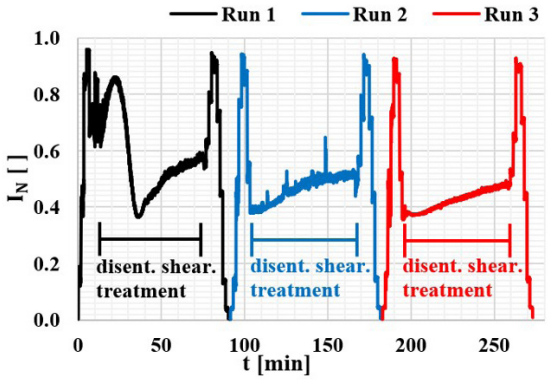

Figure 5. Changes in the normalized cross-polarized transmitted light intensity I_N as a function of time t for three sequentially applied runs of disentanglement shearing treatment of 60 min at 180 °C and $180\,s^{-1}$.

3.4 Reduction in the molecular chain orientation level during sequential runs of disentanglement shearing treatments

The effect of multiple disentanglement shearing treatments can be followed by measuring I_N as a function of time for three consecutive applied runs at 180 °C, which is shown in Figure 5. The increasing orientation with increasing shear rate $\dot{\gamma}$ is seen up to the initial 15 minutes of shearing, when $\dot{\gamma} = 180\ s^{-1}$ is reached. After that, the shear rate is kept constant at this value and the disentanglement shearing treatment takes place. At its start, $I_N = 0.65$, given a flow birefringence of $\Delta n = -23.2\times10^{-4}$. The disentanglement rate reduces over time and after 60 min of disentanglement shearing treatment, the OPD have passed by the first half of the second order and the end of the first order, reaching a $I_N = 0.57$ i.e. a flow birefringence of $\Delta n = -3.8\times10^{-4}$. After the first disentanglement shearing treatment, the shear rate is reduced down to zero, while the molecular chain orientation also reduces by chain recoiling. By applying a second run, the I_N value starts at $I_N = 0.40$ and then follows the previous behavior. During this second run, the molecular chain orientation level reduces at a much lower rate. Upon applying a third run, the whole I_N curve shape is kept very similar to that of the second run, revealing that the reduction in molecular chain orientation during disentanglement shearing treatment had already occurred mainly in the first run. After that, the molecular chain entanglement level remains constant, independent of increasing further the time of treatment, at the same shear level. The disentanglement rate is high at the beginning of the first run and stabilizes by the end of the treatment. Thus the final molecular chain relaxation is the combination of a reversible behavior due to the molecular chain uncoiling/recoiling effect, and an irreversible contribution of the molecular chain disentanglement effect.

3.5 Molecular chain orientation level after sequential disentanglement shearing treatment runs

The flow birefringence -Δn as a function of shear rates $\dot{\gamma}$ after the sample had been subjected to consecutive

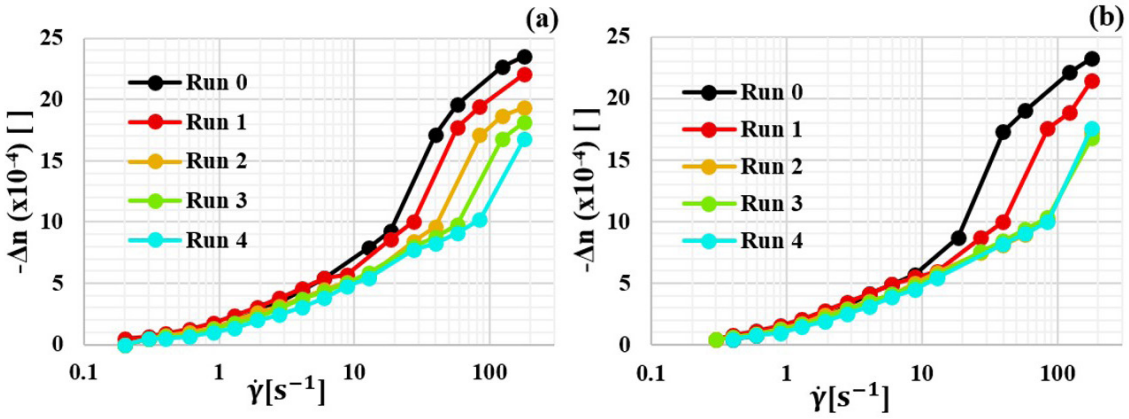

Figure 6. Flow birefringence -Δn as a function of shear rate $\dot{\gamma}$ at 180 °C for runs after disentanglement shearing treatment times of (a) 2 min and (b) 5 min.

disentanglement shearing treatment runs at 180 s^{-1} and 180℃ for 2 min and 5 min treatments are presented in Figure 6. Run 0 represents the first curve obtained while the shear rate profile is applied for the first time. The subsequent runs count the number of disentanglement shearing treatments that the sample was subjected to. In general, at low $\dot{\gamma}_s$ levels, -Δn reduces slightly, suggesting a irrelevant reduction in the chains average relaxation time λ_R. At high $\dot{\gamma}$, the shift is much more significant, indicating that the level of molecular chain orientation is more affected by disentanglement when the polymer melt is at high $\dot{\gamma}_s$. The flow birefringence curve shown during Run 1, which is done after 2 min of shearing treatment time, shifts to the right, indicating a reduction in the accumulative level of chain orientation. In the subsequent runs, there is an irreversible accumulation of disentanglement, which is also shown during runs after 5 min shearing treatment times. However, after 10 min cumulative treatment time (i.e. from Run 2 onwards), the curves overlap, indicating the stabilization of the orientation level reached by the partially disentangled chains.

The values of -Δn at 180 °C and 180 s^{-1} as a function of the accumulated disentanglement shearing treatment time after each run shown in Figure 6 were consolidated in Figure 7. There is a fast reduction of -Δn up to approximately 10 min of accumulated treatment time, subsequently leading to stability. The level of entanglement reduces with shearing treatment time, leveling after ~10 min of cumulative treatment, due to the reduction in the capacity of more disentagled chains to orient themselves.

3.6 Molecular chain orientation level as a function of melt shearing temperature

Figure 8 presents -Δn as a function of $\dot{\gamma}$ at different melt shearing temperatures without (a); and after 60 min disentanglement shearing treatment at 180 s^{-1} and 180 °C (b). In both (a) and (b) cases, Δn decreases with increasing temperature, due to reducing λ_R as the chains present greater mobility and, therefore, the $\dot{\gamma}$ necessary for the orientation to overcome the relaxation effect is greater. There is a shift to the right of (b) in relation to (a), which demonstrates the disentanglement effect. Δn are

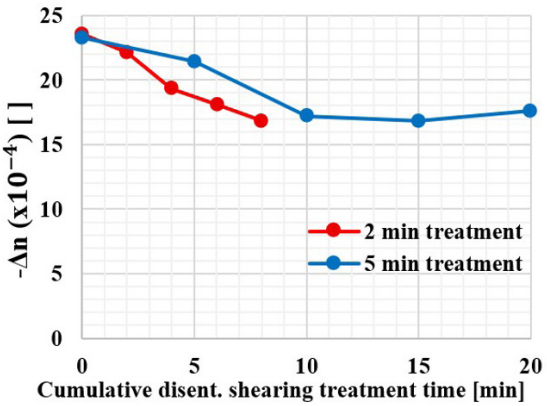

Figure 7. Flow birefringence values -Δn at 180 °C and 180 s^{-1} for consecutive runs with 2 and 5 min disentanglement shearing treatment time as a function of the cumulative treatment time.

smaller after the treatment and the same previous conclusions are valid at different temperatures.

The PS chains average relaxation times λ_R at varying melt shearing temperatures from 180 °C up to 230 °C were obtained by extrapolation the best fitting curve in the flow birefringence -Δn to zero, and calculated following Equation 5. Figure 9 shows λ_R as a function of 1/T. There is a reduction of λ_R with increasing temperature (reducing 1/T) analogous to the results obtained by Bernardo[35]. After disentanglement shearing treatment, λ_R is shifted to lower values, this effect being more pronounced at lower temperatures.

3.7 Disentanglement and recoiling model

The rheo-optical data obtained for shear melt flow of polystyrene can be represented in a model of the disentanglement and recoiling dynamics of the polymer chain in Figure 10. Polymer chains in the molten or softened state at rest are in a coiled and entangled equilibrium conformation. When subjected to shear rates high enough to overcome molecular relaxation, they uncoil and orient along the direction of stress.

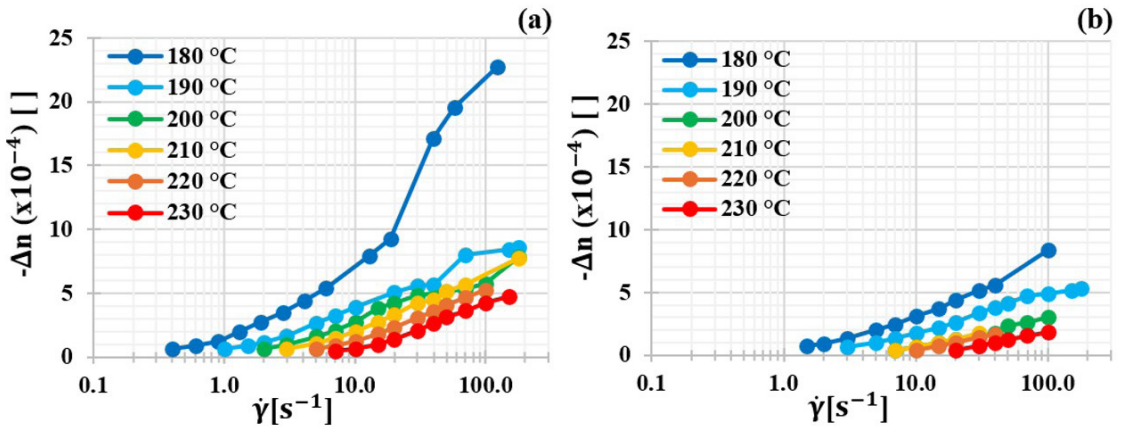

Figure 8. Flow birefringence -Δn as a function of shear rate $\dot{\gamma}$ at different temperatures (a) without; and (b) after applying 60 min disentanglement shearing treatment at 180 °C and 180 s^{-1}.

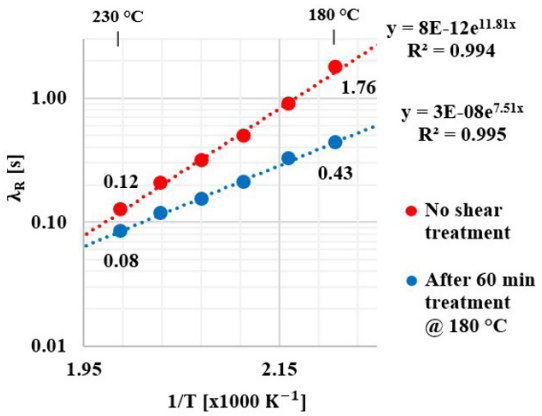

Figure 9. PS chain average relaxation times λ_R as a function of the reciprocal of the melt flow temperature 1/T, without and after applying 60 min of disentanglement shearing treatment at 180 °C.

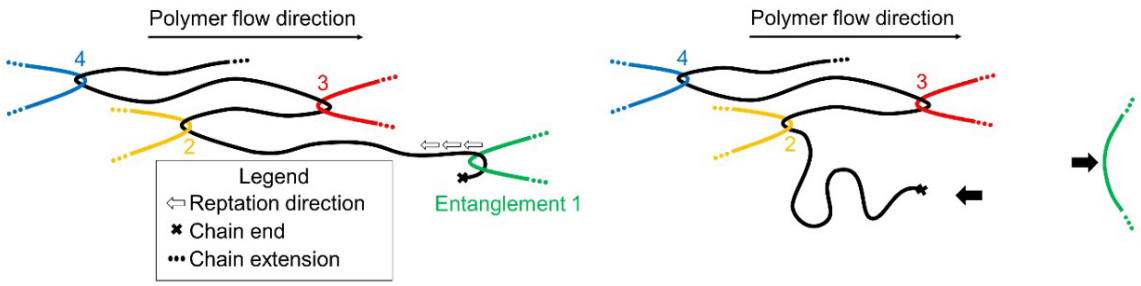

Figure 10. Dynamics of polymer chain disentanglement, recoiling and the following reduction in the molecular chain orientation level during the shearing polymer flow.

Simultaneously, there is a reduction in the entanglement level through reptation mechanisms, in agreement with recent model proposals[36-39]. An increase in the applied shear rate leads to an increase in the level of chain uncoiling and orientation. Maintaining a constant shear rate, the reptation allows entangled segments that are closer to chain ends to disentangle easier. Gradually lower levels of entanglements lead to an increase in the conformational freedom degree of the chain segment, facilitating its partial recoiling, with a gradual reduction in the level of orientation over time, analogous to the conclusions of Watanabe et al.[25] and Noirez et al.[26]. The lower orientation level reduces the ability of the chains to disentangle, as they are in a more relaxed state. Therefore, the disentanglement rate decreases over time, leading to stabilization. The disentanglement rate increases when applying higher shear rates, as the reptation speed and orientation will

be greater, in agreement with Fu et al.[30] and Liu et al.[40]. Higher temperatures reduce the disentanglement rate, as the orientation levels will be lower, due to the shorter average relaxation time. With a rapid suppression of shear, the chains recoil quickly and reversibly. However, reentanglement occurs much more slowly, as also observed by Roy and Roland[28], Ibar[29], and Litvinov et al.[41], and an irreversible effect can be assumed, within the time scale of this work.

4. Conclusions

Rheo-optical measurements quantifying polymer melt flow birefringence under controlled melt shearing conditions were carried out for a pure polystyrene of high molar mass with a Cambridge Shearing System CSS450 fitted in a polarized light optical microscope, and an optical detector to monitor the cross-polarized transmitted light intensity. With this rheo-optical setting, the level of the polymer chain orientation and its correlation with the dynamics of uncoiling/recoiling and disentanglement of the chains were studied. The expected increase in the average polymer chain orientation level with the increase in the applied shear rate due to chain uncoiling was confirmed. Under continuous shearing the average chain orientation level reduces over time, associated with the chain disentanglement, happening mainly by loosen the chain entanglements closest to the chain ends, leaving the terminal chain segments free to recoil. Under shearing, the disentanglement is irreversible, assuming that reentanglement is insignificant, while uncoiling and recoiling are reversible, depending on the level of the applied shear rate and flow temperature. A molecular model is proposed to represent these dynamics.

5. Author's Contribution

• **Conceptualization –** Murilo Tambolim; Sebastião Vicente Canevarolo.

• **Data curation –** Murilo Tambolim; Sebastião Vicente Canevarolo.

• **Formal analysis –** Murilo Tambolim; Sebastião Vicente Canevarolo.

• **Funding acquisition –** Murilo Tambolim; Sebastião Vicente Canevarolo.

• **Investigation –** Murilo Tambolim; Sebastião Vicente Canevarolo.

• **Methodology –** Murilo Tambolim; Sebastião Vicente Canevarolo.

• **Project administration –** Murilo Tambolim; Sebastião Vicente Canevarolo.

• **Resources –** Murilo Tambolim; Sebastião Vicente Canevarolo.

• **Software –** Murilo Tambolim; Sebastião Vicente Canevarolo.

• **Supervision –** Sebastião Vicente Canevarolo.

• **Validation –** Murilo Tambolim; Sebastião Vicente Canevarolo.

• **Visualization –** Murilo Tambolim; Sebastião Vicente Canevarolo.

• **Writing – original draft –** Murilo Tambolim; Sebastião Vicente Canevarolo.

• **Writing – review & editing –** Murilo Tambolim; Sebastião Vicente Canevarolo.

6. Acknowledgements

This study was financed by the Coordenação de Aperfeiçoamento de Pessoal de Nível Superior - Brasil (CAPES) - Finance Code 001, Conselho Nacional de Desenvolvimento Científico e Tecnológico (CNPq) for a PQ scholarship 310441/2020-0 to S.V. Canevarolo, and the Programa de Pós-Graduação em Ciência e Engenharia de Materiais (PPG-CEM) of Federal University of São Carlos (UFSCar).

7. References

1. Fuller, G. G., & Leal, L. G. (1981). Flow birefringence of concentrated polymer solutions in two-dimensional flows. *Journal of Polymer Science. Polymer Physics Edition*, *19*(4), 557-587. http://doi.org/10.1002/pol.1981.180190402.
2. Frattini, P. L., & Fuller, G. G. (1984). Note: a note on phase-modulated flow birefringence: a promising rheo-optical method. *Journal of Rheology (New York, N.Y.)*, *28*(1), 61-70. http://doi.org/10.1122/1.549768.
3. Zebrowski, B. E., & Fuller, G. G. (1985). Rheo-optical studies of concentrated polystyrene solutions subjected to transient simple shear flow. *Journal of Polymer Science. Polymer Physics Edition*, *23*(3), 575-589. http://doi.org/10.1002/pol.1985.180230313.
4. Silva, J., Santos, A. C., & Canevarolo, S. V. (2015). In-line monitoring flow in an extruder die by rheo-optics. *Polymer Testing*, *41*, 63-72. http://doi.org/10.1016/j.polymertesting.2014.10.007.
5. Soares, K., Santos, A. M. C., & Canevarolo, S. V. (2011). In-line rheo-polarimetry: a method to measure in real time the flow birefringence during polymer extrusion. *Polymer Testing*, *30*(8), 848-855. http://doi.org/10.1016/j.polymertesting.2011.08.007.
6. Rouse, P. E., Jr. (1953). A theory of the linear viscoelastic properties of dilute solutions of coiling polymers. *The Journal of Chemical Physics*, *21*(7), 1272-1280. http://doi.org/10.1063/1.1699180.
7. Bueche, F. (1954). Influence of rate of shear on the apparent viscosity of A-Dilute Polymer Solutions, and B-Bulk polymers. *The Journal of Chemical Physics*, *22*(9), 1570-1576. http://doi.org/10.1063/1.1740460.
8. Zimm, B. H. (1956). Dynamics of polymer molecules in dilute solution: viscoelasticity, flow birefringence and dielectric loss. *The Journal of Chemical Physics*, *24*(2), 269-278. http://doi.org/10.1063/1.1742462.
9. Peticolas, W. L. (1963). Introduction to the molecular viscoelastic theory of polymers and its applications. *Rubber Chemistry and Technology*, *36*(5), 1422-1458. http://doi.org/10.5254/1.3539650.
10. Busse, W. F. (1932). The physical structure of elastic colloids. *Journal of Physical Chemistry*, *36*(12), 2862-2879. http://doi.org/10.1021/j150342a002.
11. Treloar, L. R. G. (1940). Elastic recovery and plastic flow in raw rubber. *Rubber Chemistry and Technology*, *13*(4), 795-806. http://doi.org/10.5254/1.3546559.
12. Flory, P. J. (1944). Network structure and the elastic properties of vulcanized rubber. *Chemical Reviews*, *35*(1), 51-75. http://doi.org/10.1021/cr60110a002.

13. Buchdahl, R. (1948). Rheology of Thermoplastic Materials. I. Polystyrene. *Journal of Colloid Science*, *3*(2), 87-98. http://doi.org/10.1016/0095-8522(48)90060-9. PMid:18863839.
14. Nielsen, L. E., & Buchdahl, R. (1949). Viscoelastic and photoelastic properties of polystyrene above its softening temperature. *The Journal of Chemical Physics*, *17*(9), 839-840. http://doi.org/10.1063/1.1747411.
15. Bueche, F. (1952). Viscosity, self-diffusion, and allied effects in solid polymers. *The Journal of Chemical Physics*, *20*(12), 1959-1964. http://doi.org/10.1063/1.1700349.
16. Bueche, F. (1956). Viscosity of polymers in concentrated solution. *The Journal of Chemical Physics*, *25*(3), 599-600. http://doi.org/10.1063/1.1742998.
17. Berry, G. C., & Fox, T. G. (1968). The viscosity of polymers and their concentrated solutions. *Advances in Polymer Science*, *5*(3), 261-357. http://doi.org/10.1007/BFb0050985.
18. Onogi, S., Masuda, T., & Kitagawa, K. (1970). Rheological properties of anionic polystyrenes. I. Dynamic viscoelasticity of narrow-distribution polystyrenes. *Macromolecules*, *3*(2), 109-116. http://doi.org/10.1021/ma60014a001.
19. Gennes, P. G. (1971). Reptation of a polymer chain in the presence of fixed obstacles. *The Journal of Chemical Physics*, *55*(2), 572-579. http://doi.org/10.1063/1.1675789.
20. Ibar, J. P. (2012). Processing polymer melts under rheo-fluidification flow conditions, part 1: boosting shear-thinning by adding low frequency nonlinear vibration to induce strain softening. *Journal of Macromolecular Science, Part B: Physics*, *52*(3), 407-441. http://doi.org/10.1080/00222348.2012.711999.
21. Ibar, J. P. (2012). Processing polymer melts under rheo-fluidification flow conditions, part 2: simple flow simulations. *Journal of Macromolecular Science, Part B: Physics*, *52*(3), 442-461. http://doi.org/10.1080/00222348.2012.712004.
22. Wang, Y., Liu, M., Chen, J., Luo, J., Min, J., Fu, Q., & Zhang, J. (2020). Efficient disentanglement of polycarbonate melts under complex shear Field. *Polymer*, *201*, 122610. http://doi.org/10.1016/j.polymer.2020.122610.
23. Tapadia, P., & Wang, S.-Q. (2004). Nonlinear flow behavior of entangled polymer solutions: yieldlike entanglement-disentanglement transition. *Macromolecules*, *37*(24), 9083-9095. http://doi.org/10.1021/ma0490855.
24. Li, K., & Matsuba, G. (2017). Effects of relaxation time and zero shear viscosity on structural evolution of linear low-density polyethylene in shear flow. *Journal of Applied Polymer Science*, *135*(13), 46053. http://doi.org/10.1002/app.46053.
25. Watanabe, H., Kanaya, T., & Takahashi, Y. (2007). Rheo-SANS behavior of entangled polymer chains with local label under fast shear flow. *Activity Report on Neutron Scattering Research: Experimental Reports*, *14*, 265.
26. Noirez, L., Mendil-Jakani, H., & Baroni, P. (2009). New light on old wisdoms on molten polymers: conformation, slippage and shear banding in sheared entangled and unentangled melts. *Macromolecular Rapid Communications*, *30*(20), 1709-1714. http://doi.org/10.1002/marc.200900331. PMid:21638441.
27. Wang, Z., Lam, C. N., Chen, W.-R., Wang, W., Liu, J., Liu, Y., Porcar, L., Stanley, C. B., Zhao, Z., Hong, K., & Wang, Y. (2017). Fingerprinting molecular relaxation in deformed polymers. *Physical Review X*, *7*(3), 031003. http://doi.org/10.1103/PhysRevX.7.031003.
28. Roy, D., & Roland, C. M. (2013). Reentanglement kinetics in polyisobutylene. *Macromolecules*, *46*(23), 9403-9408. http://doi.org/10.1021/ma402074b.
29. Ibar, J. P. (2015). Trouble with polymer physics: development of "sustained orientation" contradicts the current understanding of the liquid state of polymers. *Journal of Macromolecular Science, Part B: Physics*, *54*(6), 722-748. http://doi.org/10.1080/00222348.2015.1037209.
30. Fu, J., Wang, Y., Shen, K., Fu, Q., & Zhang, J. (2019). Insight Into Shear-Induced Modification for Improving Processability of Polymers: effect of shear rate on the evolution of entanglement state. *Journal of Polymer Science. Part B, Polymer Physics*, *57*(10), 598-606. http://doi.org/10.1002/polb.24816.
31. Okada, Y., Urakawa, O., & Inoue, T. (2016). Reliability of intrinsic birefringence estimated via the modified stress-optical rule. *Polymer Journal*, *48*(11), 1073-1078. http://doi.org/10.1038/pj.2016.74.
32. Vasconcelos, R. L. (2019). *Caracterização em tempo real da birrefringência de forma do Sistema PS/PP por técnica reo-óptica* (Dissertação de mestrado). Universidade Federal de São Carlos, São Carlos.
33. Berek, M. (1913). *Compensator B Manual*. Germany: Ernst Leitz, GmbH. For the complete theory of the compensator see M. Berek (1913). Zentralblatt furr Mineralogie, pgs 388-396, 427-435, 464-470, and 580-582.
34. Vasconcelos, R. L., & Canevarolo, S. V. (2020). Rheo-optical characterization of dilute polymer mixtures under shear flow. *Polymer Testing*, *90*, 106737. http://doi.org/10.1016/j.polymertesting.2020.106737.
35. Bernardo, F. O. C. (2022). *Caracterização óptica on-line das misturas dispersiva e distributiva na extrusão dupla rosca* (Tese de doutorado). Universidade Federal de São Carlos, São Carlos.
36. Andreev, M., Khaliullin, R. N., Steenbakkers, R. J. A., & Schieber, J. D. (2013). Approximations of the discrete slip-link model and their effect on nonlinear rheology predictions. *Journal of Rheology (New York, N.Y.)*, *57*(2), 535-557. http://doi.org/10.1122/1.4788909.
37. Ianniruberto, G., & Marrucci, G. (2014). Convective constraint release (CCR) revisited. *Journal of Rheology (New York, N.Y.)*, *58*(1), 89-102. http://doi.org/10.1122/1.4843957.
38. Nafar Sefiddashti, M. H., Edwards, B. J., & Khomami, B. (2016). Steady shearing flow of a moderately entangled polyethylene liquid. *Journal of Rheology (New York, N.Y.)*, *60*(6), 1227-1244. http://doi.org/10.1122/1.4963800.
39. Dolata, B. E., & Olmsted, P. D. (2023). A thermodynamically consistent constitutive equation describing polymer disentanglement under flow. *Journal of Rheology (New York, N.Y.)*, *67*(1), 269-292. http://doi.org/10.1122/8.0000476.
40. Liu, M., Wang, Y., Chen, J., Luo, J., Fu, Q., & Zhang, J. (2020). The retarded recovery of disentangled state by blending hdpe with ultra-high molecular weight polyethylene. *Polymer*, *192*, 122329. http://doi.org/10.1016/j.polymer.2020.122329.
41. Litvinov, V., Christakopoulos, F., & Lemstra, P. J. (2024). Disentangled melt of ultrahigh-molecular-weight polyethylene: fictitious or real? *Macromolecules*, *57*(8), 3719-3730. http://doi.org/10.1021/acs.macromol.4c00271.

Received: June 14, 2024
Revised: Aug. 25, 2024
Accepted: Sept. 12, 2024